

Extensive studies of antiferromagnetic PuPd₂Sn

K. Gofryk,¹ D. Kaczorowski,² J.-C. Griveau,¹ N. Magnani,¹ R. Jardin,¹ E. Colineau,¹ J. Rebizant,¹
F. Wastin,¹ and R. Caciuffo¹

¹European Commission, Joint Research Centre, Institute for Transuranium Elements, Postfach 2340, 76125 Karlsruhe, Germany

²Institute of Low Temperature and Structure Research, Polish Academy of Sciences, P.O. Box 1410, 50-950 Wrocław, Poland

(Received 29 October 2007; published 22 January 2008)

A compound PuPd₂Sn was studied by means of x-ray diffraction, magnetization, heat capacity, electrical resistivity, magnetoresistivity, Hall effect, and thermoelectric power measurements, performed in the temperature range 2–300 K and in magnetic fields up to 14 T. This compound orders antiferromagnetically at 11 K and shows localized magnetism of Pu³⁺ ion with μ_{eff} being close to the intermediate coupling value. The total splitting of the plutonium ⁶H_{5/2} multiplet is of the order of 150 K with a doublet being the ground state. Below T_N the specific heat and the electrical resistivity are dominated by electron-magnon scattering with an antiferromagnetic spin-waves spectrum typical of anisotropic antiferromagnetic systems. Strong enhancement of the low-temperature specific heat points to the presence of conduction electrons with high effective masses. The Hall coefficient of PuPd₂Sn is positive and dominated by magnetic skew scattering. The thermoelectric power attains small positive values at high temperatures and exhibits a broad negative peak around 55 K. This behavior is discussed in terms of models appropriate for metallic systems with strong electronic correlations.

DOI: 10.1103/PhysRevB.77.014431

PACS number(s): 71.27.+a, 75.50.Ee, 75.30.Mb

I. INTRODUCTION

Actinide-based intermetallics show a wide range of correlated-electron behaviors, including magnetic ordering, nonmagnetic (Kondo) ground states, and non-Fermi liquid behavior raising a considerable interest to study the physical properties of transuranium-based compounds. Recently, this interest was even increased with the discovery of unconventional heavy fermion superconductivity in the ternaries PuCoGa₅, PuRhGa₅, and NpPd₅Al₂.^{1–3}

During the last decade, U-based compounds with the overall composition UT₂M, where T is a d-electron transition metal and M stands for a p-electron element, have attracted much attention because of their large variety of intriguing physical behaviors coming from hybridization of 5f-electronic states with s, p, and/or d electrons of their neighboring atoms. The UPd₂M ternaries crystallize with several different crystal structures^{4,5} and their magnetic and transport properties are characteristic of moderately enhanced heavy fermion antiferromagnets. For example, UPd₂In orders antiferromagnetically below $T_N=20$ K and was found to display heavy fermion features ($\gamma \approx 200$ mJ/mol K²).⁶ Moreover, it exhibits a structural phase transition at 220 K from a high-temperature cubic phase to an orthorhombic one.⁶ Two other examples are UPd₂Pb and UPd₂Sb that order antiferromagnetically at 35 and 55 K, respectively, and have been considered as heavy-fermion systems ($\gamma \approx 100$ mJ/mol K²) (Ref. 7) and $\gamma \approx 80$ mJ/mol K²,⁸ respectively). Previous studies on UPd₂Sn revealed that this compound is a nonmagnetic heavy fermion compound.^{9,10}

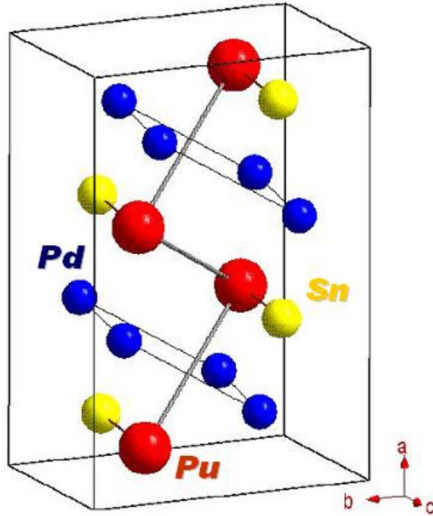
In the course of systematic investigations of the physical properties of the AnPd₂Sn family (An=Th, U, Np, and Pu)¹¹ we have already briefly reported on the antiferromagnetic compound NpPd₂Sn ($T_N=15$ K).¹² Its electrical resistivity and specific heat reveal features of a heavy-fermion ground state.¹² Here we give a full account on our studies on the synthesis, structural, and physical characterization of its Pu-

based counterpart, namely, PuPd₂Sn. The compound was examined by means of x-ray diffraction, magnetization, heat capacity, electrical resistivity, magnetoresistivity, Hall effect, and thermoelectric power measurements, performed from 2 to 300 K and in magnetic fields up to 14 T.

II. EXPERIMENTAL DETAILS

Polycrystalline samples of PuPd₂Sn were prepared by arc melting the constituents (Pu:99.8 wt %, Pd:99.999 wt %, Sn:99.999 wt %) in a Zr-gettered argon atmosphere. The weight losses during melting were less than 0.2%. Quality of the obtained material was checked at room temperature by powder x-ray diffraction using a Bruker D8 diffractometer with Cu K α_1 radiation ($\lambda=1.5406$ Å). It was revealed that the prepared sample of PuPd₂Sn was a single phase with orthorhombic *Pnma* symmetry. No extra lines were observed. The lattice parameters refined from the x-ray data are $a=10.053(9)$ Å, $b=4.502(4)$ Å, and $c=7.065(6)$ Å. Close similarities in the diffraction patterns and the values of the lattice parameters between PuPd₂Sn and the ternaries ThPd₂Sn, UPd₂Sn, and NpPd₂Sn (Refs. 9, 12, and 13) strongly suggest that the Pu-based compound is isostructural with the other materials. In this unit cell, all four atoms occupy the 4c positions ($x, \frac{1}{4}, z$), as shown in Fig. 1.

Magnetization measurements were carried out in the temperature range 2–300 K and in magnetic fields up to 7 T using a SQUID magnetometer (Quantum Design MPMS-7). The electrical resistivity, the magnetoresistivity, and the Hall effect were measured from 2 to 300 K by an ac technique employing a Quantum Design PPMS-14 platform. Heat capacity experiments were performed in the temperature range 3–300 K and in magnetic fields up to 9 T by a relaxation method using the Quantum Design PPMS-9 setup. The thermoelectric power was measured from 6 to 300 K with a homemade setup using pure copper as a reference material. The measurements of the physical properties of PuPd₂Sn

FIG. 1. (Color online) Crystal structure of PuPd₂Sn.

(even using a very small amount of the material) were limited to temperatures above 2 K due to the self-heating effect arising from the radioactive decay of the ²³⁹Pu isotope. Because of the radiotoxicity of plutonium, all experimental studies were made using special encapsulation systems to avoid contamination risks.

III. RESULTS AND DISCUSSION

A. Magnetic properties

The temperature dependence of the inverse magnetic susceptibility of PuPd₂Sn measured in an applied magnetic field of 0.5 T is shown in Fig. 2. At low temperatures a distinct minimum in the $\chi^{-1}(T)$ curve manifests the onset of antiferromagnetic ordering below the Néel temperature $T_N=11$ K. The low-temperature part of the magnetic susceptibility mea-

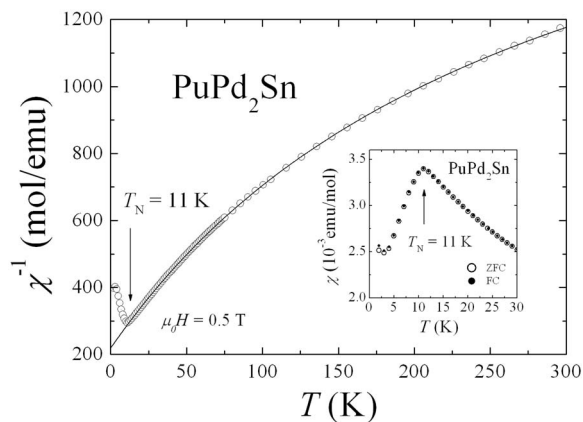


FIG. 2. Temperature dependence of the inverse magnetic susceptibility of PuPd₂Sn measured in a magnetic field $\mu_0 H=0.5$ T. The solid line is a modified Curie-Weiss fit. Inset: low-temperature part of the susceptibility measured in zero-field-cooled (ZFC) and field-cooled (FC) conditions.

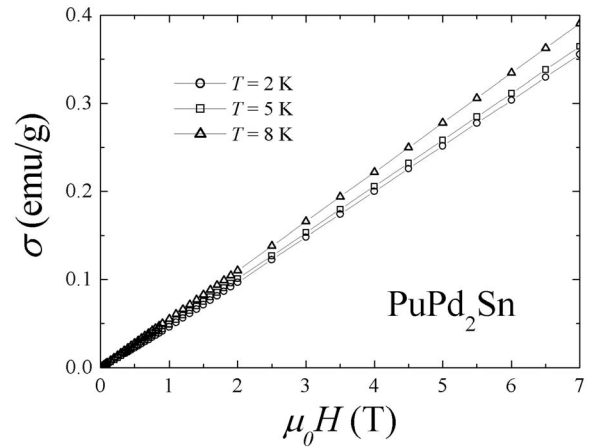


FIG. 3. Magnetization versus magnetic field of PuPd₂Sn taken at several temperatures in the ordered region.

sured in zero-field-cooled (ZFC) and field-cooled (FC) conditions is shown in the inset in Fig. 2. Above the magnetic transition, the inverse magnetic susceptibility of PuPd₂Sn is clearly curvilinear and follows a modified Curie-Weiss law as follows:

$$\chi(T) = \frac{N\mu_{eff}^2}{3k_B(T - \theta_p)} + \chi_0, \quad (1)$$

with the effective magnetic moment $\mu_{eff}=0.97\mu_B$, the paramagnetic Curie temperature $\Theta_p=-30$ K, and the Van Vleck term $\chi_0=4.8 \times 10^{-4}$ emu/mol. The experimental value of μ_{eff} is larger than the free Pu³⁺ ion value expected for Russell-Saunders coupling ($0.84\mu_B$) but it is quite close to that anticipated for intermediate coupling ($1.01\mu_B$). Interestingly, similarly to UPd₂Sn (Refs. 9 and 10) and NpPd₂Sn,¹² the absolute value of the paramagnetic Curie temperature in PuPd₂Sn is negative and strongly enhanced, as usually found in systems with strong Kondo-type interactions. Using the Hewson relation $T_K \sim \frac{|\Theta_p|}{4}$ (Ref. 14) the Kondo temperature may be estimated as 7.5 K. As shown in Fig. 3, the magnetization measured in the ordered state is proportional to the strength of the applied magnetic field with no sign of any hysteresis effect nor metamagneticlike transition up to 7 T.

B. Electrical resistivity

The temperature dependence of the electrical resistivity of PuPd₂Sn is shown in Fig. 4. At room temperature the resistivity is 121 $\mu\Omega$ cm which is the same order of magnitude observed among light actinide-based intermetallic compounds. With decreasing temperature the electrical resistivity decreases and at 2 K reaches a value around 80 $\mu\Omega$ cm.

At the magnetic phase transition, the $\rho(T)$ curve exhibits only a small kink, better seen on the temperature derivative of the resistivity $d\rho/dT$ as a pronounced positive peak of the Fisher-Langer type¹⁵ (see the inset in Fig. 4).

To estimate the magnetic contribution to the resistivity one may assume that the phonon part of the resistivity of PuPd₂Sn is the same as in its isostructural counterpart ThPd₂Sn. Thus, taking into account the experimental data of

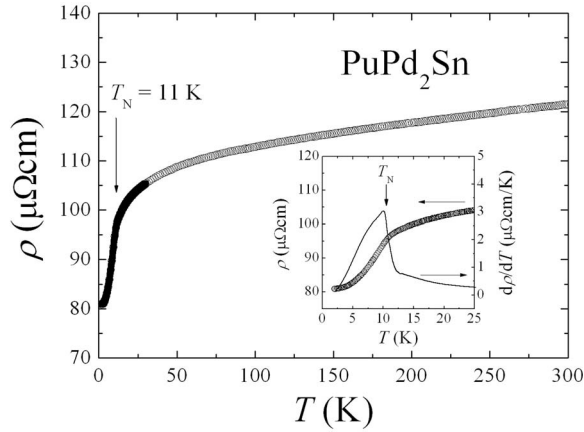


FIG. 4. Temperature dependence of the electrical resistivity of PuPd₂Sn. Inset: low-temperature variations of the resistivity (symbols) and the temperature derivative of the resistivity (solid line).

ThPd₂Sn,¹³ the magnetic contribution to the resistivity $\Delta\rho(T)$ of PuPd₂Sn can be obtained as $\Delta\rho(T)^{\text{PuPd}_2\text{Sn}} = \rho(T)^{\text{PuPd}_2\text{Sn}} - \rho(T)^{\text{ThPd}_2\text{Sn}}$, as shown in a semilogarithmic scale in Fig. 5. The general shape of the $\Delta\rho(T)$ curve with a broad maximum around 150 K, reminds the behavior of dense Kondo systems with strong crystal-field interactions. According to the theory by Cornut and Coqblin,¹⁶ the position of the maximum in $\Delta\rho(T)$ gives an estimate for the total CEF splitting. The value of 150 K is very similar to that obtained from the specific heat data (see below). At high temperatures the magnetic contribution to the electrical resistivity shows a negative logarithmic dependence characteristic of Kondo systems, as previously observed also for UPd₂Sn (Ref. 9) and NpPd₂Sn.¹² Above 150 K the $\rho(T)$ curve may be well approximated by the formula

$$\rho(T) = \rho_0 + \rho_0^\infty + c_K \ln T, \quad (2)$$

appropriate for scattering of conduction electrons by defects and imperfections in the crystal lattice, disordered spins, and Kondo impurities, respectively. Least-squares fit of this expression to the experimental data yields the parameters ($\rho_0 + \rho_0^\infty$) = 111 $\mu\Omega$ cm and c_K = -1.1 $\mu\Omega$ cm.

Below the magnetic phase transition the electrical resistivity of PuPd₂Sn may be well described by the model proposed by Continentino *et al.*^{17,18} which takes into account scattering processes of conduction electrons on the antiferromagnetic spin waves with a gap in the magnon spectrum. Assuming that the dispersion of antiferromagnetic magnons can be approximated by the relation $\omega = \sqrt{\Delta^2 + Dk^2}$, in which Δ is the spin-wave gap while D stands for the spin-waves stiffness, the electrical resistivity may be expressed as^{17,18}

$$\rho(T) = \rho_0 + b\Delta^2 \sqrt{\frac{k_B T}{\Delta}} e^{-\Delta/k_B T} \left[1 + \frac{3\Delta}{2k_B T} + \frac{2}{15} \left(\frac{\Delta}{k_B T} \right)^2 \right], \quad (3)$$

where the coefficient b is defined as $b \propto D^{-3/2}$. Below 9 K, least-squares fitting of Eq. (3) to the experimental data of PuPd₂Sn give the following parameters, ρ_0 = 81 $\mu\Omega$ cm, b

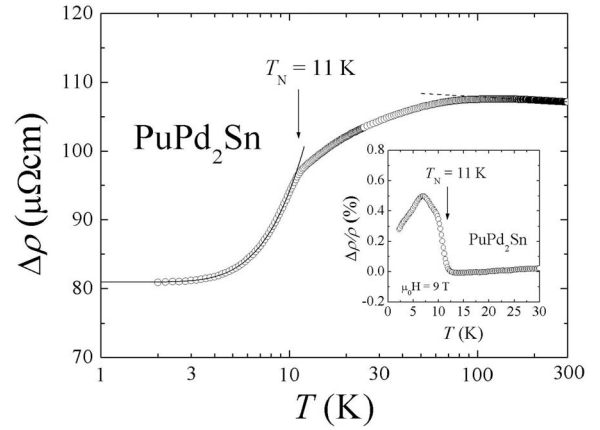


FIG. 5. Temperature dependence of the magnetic contribution to the electrical resistivity of PuPd₂Sn. The solid and dashed lines are fits using expressions given in the text. Inset: temperature variation of the magnetoresistivity.

= 0.28 $\mu\Omega$ cm/K², and Δ = 12 K. From the evaluation of the resistivity data in terms of Eqs. (2) and (3) the spin-disorder resistivity ρ_0^∞ in PuPd₂Sn is estimated to be about 30 $\mu\Omega$ cm.

The temperature dependence of the transverse ($\mu_0 \vec{H} \perp \vec{i}$) magnetoresistivity (MR), defined as $\frac{\Delta\rho}{\rho} = \frac{\rho(B) - \rho(0)}{\rho(0)}$ and measured in an applied magnetic field $\mu_0 H = 9$ T, is shown in the inset in Fig. 5. The magnetoresistivity is very small and reaches a maximum value of about 0.5% at 6 K. The overall shape of the MR(T) curve is characteristic of antiferromagnets, as theoretically predicted by Yamada and Takeda.¹⁹

C. Hall effect

Figure 6 shows the temperature dependence of the Hall coefficient of PuPd₂Sn. At room temperature the Hall constant is positive and of the order of 0.5×10^{-10} m³ C⁻¹. With decreasing temperature, it continuously increases down to the Néel temperature $T_N = 11$ K, at which the $R_H(T)$ curve

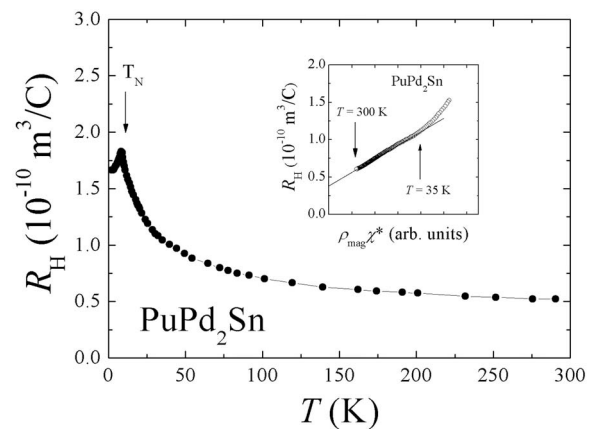


FIG. 6. Temperature dependence of the Hall coefficient of PuPd₂Sn measured in magnetic field $B = 14$ T. Inset: R_H vs $\chi^* \rho_{\text{mag}}$ (see the text). The solid line is a fit of Eq. (4) to the experimental data.

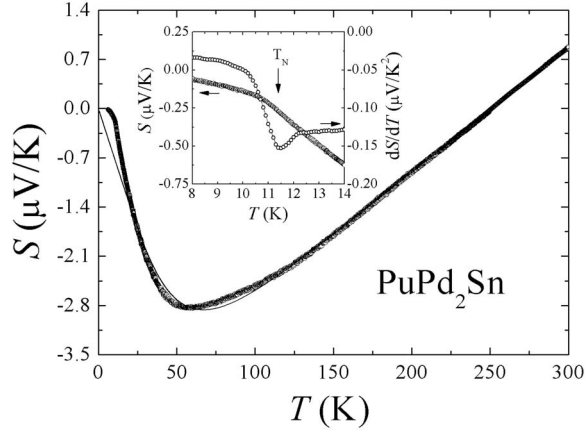


FIG. 7. Temperature dependence of the thermoelectric power of PuPd_2Sn . The solid line is a fit of Eq. (10) to the experimental data. Inset: the Seebeck coefficient and temperature dependence of the derivative of the thermopower in the vicinity of the magnetic phase transition.

displays a distinct maximum, reminiscent of the anomaly in the temperature variation of the magnetic susceptibility.

According to the theory by Fert and Levy,²⁰ the temperature dependence of the Hall coefficient of a Kondo lattice (above the Kondo temperature) may be expressed as

$$R_H(T) = R_0 + \gamma_1 \chi^*(T) \rho_{mag}(T), \quad (4)$$

where the first term describes the Hall effect due to Lorentz motion of carriers and/or residual skew scattering by defects and impurities, while the second term comes from intrinsic skew scattering by Kondo impurities. In this formula $\chi^*(T)$ is a reduced susceptibility being approximated by $\chi(T)/C$, where C is the Curie-Weiss constant, whereas $\rho_{mag}(T)$ is the magnetic contribution to the electrical resistivity. In the case of PuPd_2Sn , least-squares fitting of Eq. (4) to the experimental data in the temperature range 35–300 K (see the inset in Fig. 6) resulted in the values $R_0 = 3.9 \times 10^{-11} \text{ m}^3/\text{C}$ and $\gamma_1 = 3.1 \times 10^{-3} \text{ K/T}$. The so-obtained γ_1 value is about ten times larger than the one obtained for cerium-based heavy fermion compounds CeCu_6 , CeAl_3 (Ref. 20), or for monocrystalline Ce_2PdSi_3 .²¹ The value of the ordinary Hall coefficient R_0 has in PuPd_2Sn a magnitude similar to that obtained in its nonmagnetic counterpart ThPd_2Sn .¹³ A simple one-band model provides an estimate for the concentration of free holes to be $1.6 \times 10^{23} \text{ cm}^{-3}$, which should be considered as the upper limit of the actual carrier concentration in PuPd_2Sn .

D. Thermoelectric power

The temperature dependence of the Seebeck coefficient of PuPd_2Sn is displayed in Fig. 7. At room temperature the thermopower is about $+1 \mu\text{V/K}$. With decreasing temperature the Seebeck coefficient decreases, changes sign at about 250 K, and shows a broad minimum of about $-2.8 \mu\text{V/K}$ near 50 K. Similarly to the electrical resistivity, the magnetic phase transition manifests itself only as a small kink on the $S(T)$ curve. It is better seen as a pronounced minimum on the

temperature derivative of the thermopower dS/dT (see the inset in Fig. 7). The total change in the thermoelectric power is quite small, thus consistent with the metallic character of the electrical resistivity. Above 150 K, the Seebeck coefficient shows a linear T dependence, which may indicate that the diffusion contribution to the total thermopower dominates the scattering at high temperatures. Generally, this mechanism may be expressed as²²

$$S(T) = \frac{k_B^2 \pi^2 T}{3|e|E_F} \left[\frac{\partial \ln n(E)}{\partial \ln E} + \frac{\partial \ln v^2(E)}{\partial \ln E} + \frac{\partial \ln \tau(E)}{\partial \ln E} \right], \quad (5)$$

where $n(E)$, $v(E)$, and $\tau(E)$ denote the density of states, the velocity of carriers, and the relaxation time of carriers, respectively, near the Fermi level. Consequently, the thermoelectric power is very sensitive to details of the electronic band structure, especially in compounds with narrow bands near E_F . Hence, in strongly correlated electron systems complicated temperature dependencies of the Seebeck coefficient with pronounced maxima or minima are frequently observed. To describe the temperature variations of the Seebeck coefficient in such compounds a simple phenomenological model was developed,²³ which takes into account scattering processes of conduction electrons from broad s - d bands into a narrow $4f$ or $5f$ quasiparticle band. The latter band is assumed to have a Lorentzian form

$$n(E) = \frac{W}{\varepsilon_F^2 + W^2}, \quad (6)$$

where W denotes its width and ε_F is its position with respect to the Fermi energy. The model predicts the following temperature dependence of the Seebeck coefficient:^{23,24}

$$S(T) = \frac{2\pi^2 k_B}{3|e|} \frac{\varepsilon_F T}{\frac{\pi^2 T^2}{3} + \varepsilon_F^2 + W^2}, \quad (7)$$

in agreement with the behavior of many Ce- and U-based heavy fermion compounds.^{8,24–26}

The so-called two-band model is found sometimes to be insufficient to properly describe the thermopower of some strongly correlated electron systems (see, e.g., Ref. 27). To overcome the problems Freimuth proposed²⁸ to consider possible variations with temperature of the parameters W and ε_F as follows:

$$\varepsilon_F = A + B e^{-T_m/T}, \quad (8)$$

and

$$W = T_f e^{-T_f/T}, \quad (9)$$

where A , B , and T_m are sample-dependent constants, while the parameter T_f is related to the quasielastic linewidth of the Kondo peak and can be directly obtained by means of inelastic neutron scattering experiments.²⁹ With this modification the formula for the Seebeck coefficient reads as follows:^{28,30}

$$S(T) = C_1 T + \frac{C_2 T \varepsilon_F(T)}{\varepsilon_F(T)^2 + W(T)^2}, \quad (10)$$

where C_1 and C_2 are temperature-independent parameters that determine the strength of the contributions arising from the nonmagnetic Mott-type [see Eq. (5)] and the magnetic scattering processes, respectively. The above expression was successfully applied to describe $S(T)$ variations of several cerium-, ytterbium-, and uranium-based heavy-fermion systems.^{27,28,30,31} As shown in Fig. 7 it provides also a quite good approximation of the thermoelectric power of PuPd₂Sn nearly in the entire temperature range studied. In the performed analysis it was assumed, like in the original paper by Freimuth,²⁸ that T_m is equal to zero, and thus the position of the Kondo peak is independent of temperature. The least-squares fit of Eq. (10) to the experimental data yielded the parameters $C_1 = 0.06 \mu\text{V}/\text{K}^2$, $C_2 = -6.34 \mu\text{V}/\text{K}$, $\varepsilon_F = 49 \text{ K}$, and $T_f = 69 \text{ K}$, which are similar to those derived for 4*f*- and 5*f*-electron-based compounds with strong correlations.

The aforesaid models are very simple and neglect some important interactions present in the crystalline solids. A more reliable approach should take into account electric field effect (CEF) and its influence on the electronic band structure. In the model by Coqblin and Schrieffer (CS)^{32,33} the Kondo effect is described in the presence of the crystal-field interactions, which strongly influence the temperature variations of the Seebeck coefficient. In particular, a characteristic broad extremum in $S(T)$ is predicted to occur at $T_{ext} \approx \frac{\Delta}{3}$, where Δ denotes the total crystal-field splitting. In the case of PuPd₂Sn the minimum in $S(T)$ is located around 55 K which implies $\Delta = 165 \text{ K}$ being consistent with the result obtained from the specific heat and magnetic susceptibility data. Recently, Zlatić *et al.* extended the CS model by considering, besides the crystal-field interactions, hybridization effect between the 4*f* and conduction electrons.^{34–37} The latter model was successfully applied to describe the temperature dependencies of the thermoelectric power in CeCu₂Si₂ (Ref. 35) and CeRu₂Ge₂,^{38,39} as well as the $S(T)$ behavior under hydrostatic pressure.

Finally, it should be noted that the magnitude of the Seebeck coefficient in PuPd₂Sn is much smaller than the thermopower values usually found for strongly correlated electron systems. A possible explanation of this discrepancy is that the thermopower is reduced because of the presence of some disorder in the crystal lattice caused by radioactive decay of the ²³⁹Pu isotope. It gives a ²³⁵U recoil atom and an alpha particle inducing disorder in the lattice.⁴⁰ Furthermore, similar small values of the Seebeck coefficient were observed in disordered Kondo lattices such as, for example, Ce₂NiGe₃.⁴¹

E. Heat capacity

Figure 8 shows the temperature dependence of the specific heat of PuPd₂Sn. Near room temperature C_p has a value of about 100 J/mol K that corresponds to the Dulong-Petit limit, i.e., $C_p = 3nR = 99.77 \text{ J/mol K}$, where n is the number of atoms per molecule and R is the gas constant. The magnetic phase transition at $T_N = 11 \text{ K}$ manifests itself as a small

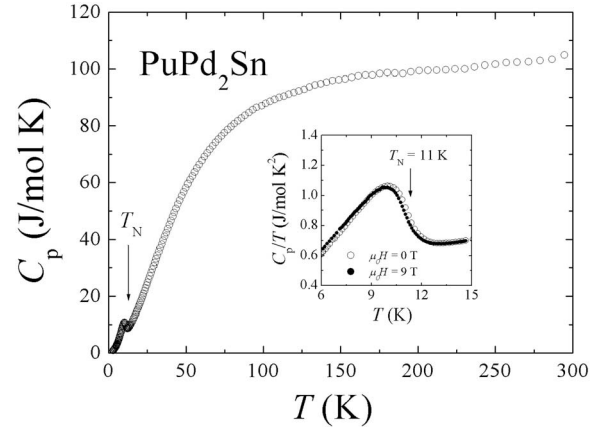


FIG. 8. Temperature dependence of the specific heat of PuPd₂Sn. Inset: temperature variation near T_N of the ratio C_p/T measured in zero magnetic field and in a field of 9 T.

λ -type anomaly in $C_p(T)$. This peak is hardly affected by an applied magnetic field. As shown in the inset in Fig. 8 in a field as strong as 9 T, the maximum in C_p/T shifts only faintly towards lower temperature and insignificantly decreases in magnitude. The observed behavior is very similar to that found before for NpPd₂Sn.¹²

The electronic contribution to the specific heat of PuPd₂Sn is strongly enhanced at low temperatures. The C_p/T ratio extrapolated to $T=0 \text{ K}$ from the regions above and below T_N is as large as 570 mJ/mol K⁻² and 180 mJ/mol K⁻², respectively (cf. Ref. 11). These values are comparable with the Sommerfeld coefficients reported for UPd₂Sn and NpPd₂Sn, which were 130 mJ/mol K⁻² (Ref. 10) and 400 mJ/mol K⁻²,¹² respectively.

In order to estimate the magnetic contribution to the specific heat of PuPd₂Sn one may assume that the phonon part to the total specific heat of PuPd₂Sn is similar to that in its isostructural counterpart ThPd₂Sn containing no 5*f* electrons. The excess specific heat calculated as $\Delta C(T) = C_p(T)^{\text{PuPd}_2\text{Sn}} - C(T)_{ph}^{\text{ThPd}_2\text{Sn}}$ (here our unpublished $C(T)_{ph}^{\text{ThPd}_2\text{Sn}}$ data were used¹³) is shown in Fig. 9.

Below the magnetic phase transition $\Delta C(T)$ can be well approximated by the formula

$$\Delta C(T) = \gamma^* T + C_{mag}(T), \quad (11)$$

where the first term describes the electronic contribution due to heavy electrons and the second one is appropriate for excitations of antiferromagnetic spin waves over a gap ΔT in the magnon spectrum^{18,42} as follows:

$$C_{mag}(T) = c\Delta^{7/2}\sqrt{T}e^{-\Delta/T}\left[1 + \frac{39T}{20\Delta} + \frac{51}{32}\left(\frac{T}{\Delta}\right)^2\right]. \quad (12)$$

In this expression the same dispersion relation of magnons was assumed as that applied above in the analysis of the electrical resistivity, and the coefficient c is related to the spin-wave stiffness D being defined as $c \propto D^{-3}$. The least-squares fit of Eq. (11) to the experimental data below 8 K, shown by the solid line in Fig. 9, yielded the parameters $\gamma^* = 161 \text{ mJ/mol K}^2$, $c = 11 \times 10^{-4} \text{ J/mol K}^4$, and $\Delta = 7 \text{ K}$.

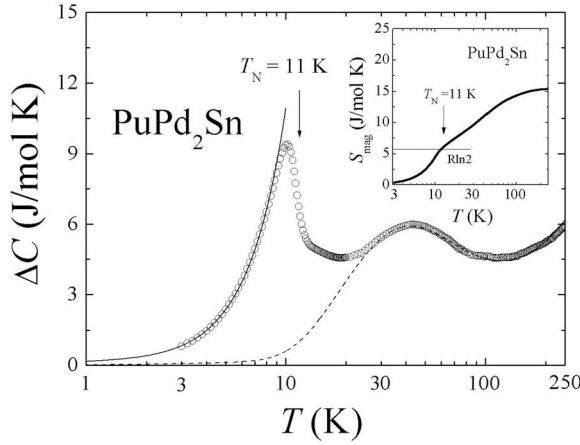


FIG. 9. Temperature dependence of the magnetic contribution to the specific heat of PuPd₂Sn (note a semilogarithmic scale). The solid and dashed lines are fits described in the text. The inset displays the temperature variation of the magnetic entropy.

The so-obtained value of the magnon gap is reasonable with respect to the Néel temperature and similar to that derived from the electrical resistivity data (see above). It is also worthwhile noting that the Δ and c values are similar to those derived for cerium-based heavy fermion systems such as CeCoGe_{3-x}Si_x (Refs. 18 and 42) or CeNiGe₃.⁴³

At T_N the specific heat exhibits a jump δC of about 7 J/mol K. In dense Kondo systems the magnitude of this jump is given by^{44,45}

$$\delta C = \frac{6Rk_B}{\psi'''\left(\frac{1}{2} + \zeta\right)} \left[\psi'\left(\frac{1}{2} + \zeta\right) + \zeta\psi''\left(\frac{1}{2} + \zeta\right) \right]^2, \quad (13)$$

where $\zeta = \frac{T_K}{2\pi T_N}$, whereas ψ' , ψ'' , and ψ''' are the first, second, and third derivative of digamma function, respectively. Within this simple approach, formulated within the mean-field approximation, the Kondo temperature in PuPd₂Sn is estimated to be about 8 K.

Another estimate for T_K comes from the analysis of the magnetic entropy that is released at the Néel temperature. As shown in the inset in Fig. 9 the entropy in PuPd₂Sn reaches at T_N a value of about 91% of $R \ln 2$. By applying the formula⁴⁶

$$\frac{\Delta S}{R} = \ln(1 + e^{-T_K/T_N}) + \frac{T_K}{T_N} \frac{e^{-T_K/T_N}}{1 + e^{-T_K/T_N}}, \quad (14)$$

adequate for dense Kondo systems, one finds $T_K \approx 7.6$ K. It is worth noting that the two values of T_K derived from the specific heat data are close to one another and agree well with the value $T_K = 7.5$ K estimated from the magnetic susceptibility characteristics (see above).

In the paramagnetic region of PuPd₂Sn, the overall shape of the $\Delta C(T)$ curve, with a pronounced Schottky-type maximum near 44 K, indicates a predominant contribution due to crystal-field effect. The dashed line in Fig. 9 represents the sum of the electronic and Schottky terms, $\Delta C(T) = \gamma_{HT}T + C_{CEF}(T)$, where the Pu³⁺ ground multiplet is split into three

doublets. The least-squares fitting yielded the parameter γ_{HT} of about 23 J/mol K² and energies of the excited states $\Delta_1 = 70$ K and $\Delta_2 = 150$ K. In this context it is worthwhile noting that the magnetic entropy in PuPd₂Sn reaches at T_N a value of 5.3 J/mol K (see the inset in Fig. 9) that is close to $R \ln 2$, expected for a doublet ground state. In turn, at high temperatures the entropy saturates at a value of about 15 J/mol K, which is nearly equal to $R \ln 6$ which corresponds to the sixfold degeneracy of the Pu³⁺ ground multiplet.

F. Crystal-field analysis

The effective magnetic moment calculated from the magnetic susceptibility data of PuPd₂Sn is $\mu_{eff} = 0.97\mu_B$ (see above), i.e., it is very close to that predicted for the $J=5/2$ ground state of the $5f^5$ electronic configuration of Pu³⁺ ions when intermediate coupling is taken into account ($1.01\mu_B$). This finding clearly points towards an essentially localized behavior of the $5f$ electrons in this compound, which should be well describable within a crystalline electrical field (CEF) approach, as, for example, the magnetic behavior in the $AnPd_3$ ($An=U, Np, Pu$) series of compounds, and in particular, the properties of UPd₃, which is known as a rare example of a fully localized uranium-based intermetallic system.⁴⁷ As the tendency to localization generally grows with the atomic number within the actinide series, the hypothesis that the magnetic properties of PuPd₂Sn can be understood within a crystal-field model seems well grounded.

The Hamiltonian describing the quantum states of an actinide ion with $5f^N$ electronic configuration and well-localized electrons can be written as the sum of free-ion and CEF parts.⁴⁸ The free-ion parameters for Pu³⁺ can be found, e.g., in Ref. 49. The orthorhombic symmetry conditions impose the CEF Hamiltonian to have the form

$$H_{CF} = \sum_{k=1}^3 \sum_{q=0}^k B_{2k}^{2q} (C_{2k}^{-2q} + C_{2k}^{2q}), \quad (15)$$

where C_{2k}^{2q} are the CEF operators defined in accord with the Wybourne normalization.⁴⁸ In principle, nine nonzero CEF parameters B_{2k}^{2q} are allowed, however, most of them have very limited effect on the energy spectra and wave-function composition, as long as a sixfold-degenerate ground multiplet is considered (separated from the next higher manifold by about 4700 K). In fact, the matrix elements of sixth-order C_6^{2q} operators within two states with $J=5/2$ are all zero because the triangular inequality for the Wigner $3j$ symbols is not satisfied.⁵⁰ Moreover, the Stevens factor β (which enters as a proportionality factor in the explicit expression of fourth-order B_4^{2q} CF parameters),⁵¹ calculated for the Pu³⁺ ion in the intermediate coupling regime, ($\beta_{IC} \approx -2.4 \times 10^{-4}$) is one order of magnitude smaller in size than the Russell-Saunders approximation for a $5f^5$ electronic configuration,⁵¹ while the second-order Stevens factor α is only slightly affected. These considerations suggest that only the second-order CEF parameters, i.e., B_2^0 and B_2^2 , have significant impact on the energy spectra of Pu³⁺. The presence of J -mixing effects does not change the situation, and it has been shown⁵² that the use of Stevens operators with renormalized values of

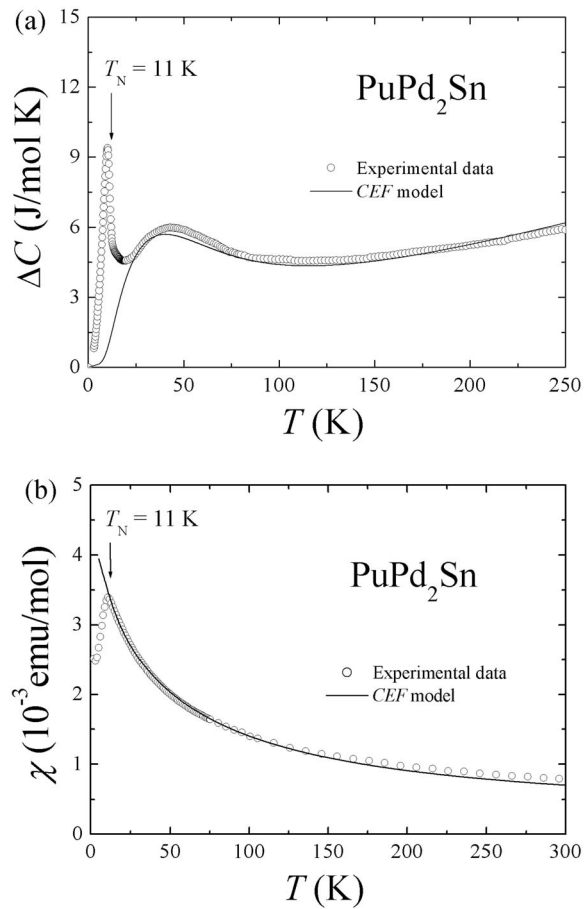


FIG. 10. Temperature dependence of the magnetic contribution of the specific heat (a) and the magnetic susceptibility (b) of PuPd₂Sn. The solid lines are fits described in the text.

the parameters can correctly take it into account. Nevertheless, this hypothesis was checked by numerical diagonalization of the full matrix for the $5f^5$ configuration and found to hold very well if fourth- and sixth-order parameters are varied within a reasonable range.

Based on the above arguments the magnetic specific heat curve of PuPd₂Sn was fitted above T_N by varying the second-order CEF parameters only. In this analysis the electronic contribution to the specific heat was taken into account by adding a term in the form $C_{el} = \gamma_{HT}T$. The best fit, shown by the solid line in Fig. 10(a), yielded the parameters $B_2^0 = 330$ K and $B_2^2 = 97$ K, and resulted in a doublet-doublet-doublet CEF scheme with the first and second excited doublets being located above the ground level at 64 and 146 K, respectively. These values of the CEF parameters were then used to calculate the magnetic susceptibility in the paramagnetic state χ_p . The contribution due to antiferromagnetic exchange interaction was taken into account according to the formula $\chi^{-1} = \chi_p^{-1} + \lambda$. As shown in Fig. 10(b), the calculated magnetic susceptibility curve compares very well to the experimental one if one chooses $\lambda^{-1} = 4.6 \times 10^{-3}$ emu/mol. We recall that the antiferromagnetic ordering condition is satisfied if $\lambda^{-1} = \chi_{p,\zeta}(T_N)$, where ζ is the direction of the magnetic moments in the ordered phase. Though some ambiguity in

the choice of the reference frame is always present when dealing with orthorhombic symmetry,⁵³ the model provides for PuPd₂Sn a value $\chi_{p,z}(T_N) \approx 1.7 \times 10^{-3}$ emu/mol along the “easy” z axis. While the order of magnitude of $\chi_{p,z}(T_N)$ is the same as of λ^{-1} , the apparent discrepancy between the two values may be due to the presence of more complex features not accounted for by the model applied, such as anisotropic superexchange interactions. Direct spectroscopic measurements of the energy spectra, for example, by means of inelastic neutron scattering, and precise determination of the antiferromagnetic structure in the ordered phase would be crucial to further investigate this point.

IV. SUMMARY AND CONCLUSIONS

The Pu-based intermetallic compound PuPd₂Sn was synthesized and thoroughly studied in wide temperature and magnetic field ranges. The compound crystallizes, like other members of the $AnPd_2Sn$ series with $An = Th, U, \text{ and } Np$, in the orthorhombic $Pnma$ unit cell. The magnetic measurements revealed that PuPd₂Sn orders antiferromagnetically at $T_N = 11$ K. From the specific heat, magnetic susceptibility, and resistivity data the crystal-field splitting of the Pu⁺³ multiplet was estimated to be about 150 K, with a doublet being the ground state and two other doublets being the excited states. The large negative paramagnetic Curie temperature (with respect to the Néel temperature), negative logarithmic slope of the magnetic contribution to the resistivity, and strongly enhanced low-temperature electronic specific heat are all indicative that PuPd₂Sn belongs to a family of dense Kondo systems with heavy-fermion ground state. Using a few different approaches, the Kondo temperature was estimated to be of about 7 K. Also the temperature dependencies of the Hall coefficient and the thermoelectric power, determined for PuPd₂Sn, are typical for intermetallics with strong electronic correlations. The positive sign of both the ordinary Hall coefficient and the thermopower at high temperatures indicates that the charge and heat transport in the compound studied is likely dominated by hole carriers.

To summarize, the observed physical behavior in PuPd₂Sn strongly suggests that it may be a heavy-fermion system, one of very few known so far amidst plutonium-based intermetallics.⁵⁴ However, despite the obtained coherent description of this compound in terms of Kondo interactions, some ambiguity still remains, especially in the analysis of the Seebeck coefficient. Therefore, further studies are required on the electronic ground state, possibly using less disordered material. One possibility would be to synthesize PuPd₂Sn using ²⁴²Pu to decrease self-decay and hence reduce disorder effect.

ACKNOWLEDGMENTS

This work was made possible thanks to the support of the European Community-Access to Research Infrastructures action of the Improving Human Potential Programme in financing the access to the Actinide User Laboratory at the

ITU-Karlsruhe under Contract No. RITA-CT-2006-026176-“Actuslab-2.” High purity Pu metal was made available through a loan agreement between Lawrence Livermore National Laboratory, and ITU, in the frame of a collaboration

involving LLNL, Los Alamos National Laboratory, and the U.S. Department of Energy. K.G. acknowledges the European Commission for support in the frame of the “Training and Mobility of Researchers” programme.

- ¹J. L. Sarrao, L. A. Morales, J. D. Thompson, B. L. Scott, G. R. Stewart, F. Wastin, J. Rebizant, P. Boulet, E. Colineau, and G. H. Lander, *Nature (London)* **420**, 297 (2002).
- ²F. Wastin, P. Boulet, J. Rebizant, E. Colineau, and G. H. Lander, *J. Phys.: Condens. Matter* **15**, 2279 (2003).
- ³D. Aoki, Y. Haga, T. D. Matsuda, N. Tateiwa, S. Ikeda, Y. Homma, H. Sakai, Y. Shiokawa, E. Yamamoto, A. Nakamura, R. Settai, and Y. Ōnuki, *J. Phys. Soc. Jpn.* **76**, 063701 (2007).
- ⁴Z. Żolnierek, *J. Magn. Magn. Mater.* **76-77**, 231 (1988).
- ⁵M. Marezio, D. E. Cox, C. Rossel, and M. B. Maple, *Solid State Commun.* **67**, 831 (1988).
- ⁶T. Takabatake, H. Kawanaka, H. Fujii, Y. Yamaguchi, J. Sakurai, Y. Aoki, and T. Fujita, *J. Phys. Soc. Jpn.* **58**, 1918 (1998).
- ⁷C. L. Seaman, N. R. Dilley, M. C. deAndrade, J. Herrmann, M. B. Maple, and Z. Fisk, *Phys. Rev. B* **53**, 2651 (1996).
- ⁸K. Gofryk, D. Kaczorowski, and A. Czopnik, *Solid State Commun.* **133**, 625 (2005).
- ⁹C. Rossel, M. S. Torikachvilli, J. W. Chen, and M. B. Maple, *Solid State Commun.* **60**, 563 (1986).
- ¹⁰I. Maksimov, F. J. Litterst, H. Rechenberg, M. A. C. de Melo, R. Feyerherm, R. W. A. Hendriks, T. J. Gortenmulder, J. A. Mydosh, and S. Süllow, *Phys. Rev. B* **67**, 104405 (2003).
- ¹¹K. Gofryk, D. Kaczorowski, E. Colineau, F. Wastin, R. Jardin, J.-C. Griveau, N. Magnani, J. Rebizant, P. Boulet, P. Javorský, and R. Caciuffo, *Physica B* (to be published).
- ¹²D. Kaczorowski, K. Gofryk, P. Boulet, J. Rebizant, P. Javorský, E. Colineau, F. Wastin, and G. H. Lander, *Physica B* **359-361**, 1102 (2005).
- ¹³K. Gofryk *et al.* (unpublished).
- ¹⁴A. C. Hewson, *The Kondo Problem to Heavy Fermions* (Cambridge University Press, Cambridge, 1993).
- ¹⁵M. E. Fisher and J. S. Langer, *Phys. Rev. Lett.* **20**, 665 (1968).
- ¹⁶D. Cornut and B. Coqblin, *Phys. Rev. B* **5**, 4541 (1972).
- ¹⁷M. B. Fontes, J. C. Trochez, B. Giordanengo, S. L. Budko, D. R. Sanchez, E. M. Baggio-Saitovitch, and M. A. Continentino, *Phys. Rev. B* **60**, 6781 (1999).
- ¹⁸S. N. de Medeiros, M. A. Continentino, M. T. D. Orlando, M. B. Fontes, E. M. Baggio-Saitovitch, A. Rosch, and A. Eichler, *Physica B* **281-282**, 340 (2000).
- ¹⁹H. Yamada and S. Takeda, *J. Phys. Soc. Jpn.* **34**, 51 (1973).
- ²⁰A. Fert and P. M. Levy, *Phys. Rev. B* **36**, 1907 (1987).
- ²¹S. R. Saha, H. Sugawara, T. D. Matsuda, Y. Aoki, H. Sato, and E. V. Sampathkumaran, *Phys. Rev. B* **62**, 425 (2000).
- ²²R. D. Bernard, *Thermoelectricity in Metals and Alloys* (Taylor and Francis LTD, London, 1972).
- ²³U. Gottwick, K. Gloss, S. Horn, F. Steglich, and N. Grewe, *J. Magn. Magn. Mater.* **77-78**, 536 (1985).
- ²⁴M. D. Koterlyn, O. I. Babych, and G. M. Koterlyn, *J. Alloys Compd.* **325**, 6 (2001).
- ²⁵Y. Bando, T. Suemitsu, K. Takagi, H. Tokushima, Y. Echizen, K. Katoh, K. Umeo, Y. Maeda, and T. Takabatake, *J. Alloys Compd.* **313**, 1 (2000).
- ²⁶A. P. Pikul, D. Kaczorowski, Z. Bukowski, K. Gofryk, U. Burkhardt, Yu. Grin, and F. Steglich, *Phys. Rev. B* **73**, 092406 (2006).
- ²⁷D. Kaczorowski and K. Gofryk, *Solid State Commun.* **138**, 337 (2006).
- ²⁸A. Freimuth, *J. Magn. Magn. Mater.* **68**, 28 (1987).
- ²⁹E. Holland-Moritz, D. Wohlleben, and M. Loewenhaupt, *Phys. Rev. B* **25**, 7482 (1982).
- ³⁰C. S. Garde and J. Ray, *Phys. Rev. B* **51**, 2960 (1995).
- ³¹V. H. Tran, R. Troć, Z. Bukowski, D. Badurski, and C. Sułkowski, *Phys. Rev. B* **71**, 094428 (2005).
- ³²B. Coqblin and J. R. Schrieffer, *Phys. Rev.* **185**, 847 (1969).
- ³³K. Bhattacharjee and B. Coqblin, *Phys. Rev. B* **13**, 3441 (1976).
- ³⁴V. Zlatić, I. Milat, B. Coqblin, and G. Czycholl, *Physica B* **312-313**, 171 (2002).
- ³⁵V. Zlatić, B. Horvatić, I. Milat, B. Coqblin, G. Czycholl, and C. Grenzebach, *Phys. Rev. B* **68**, 104432 (2003).
- ³⁶V. Zlatić and R. Monnier, *Phys. Rev. B* **71**, 165109 (2005).
- ³⁷V. Zlatić, R. Monnier, J. Freericks, and K. W. Becker, *Phys. Rev. B* **76**, 085122 (2007).
- ³⁸H. Wilhelm, D. Jaccard, V. Zlatić, R. Monnier, B. Delley, and B. Coqblin, *J. Phys.: Condens. Matter* **17**, S823 (2005).
- ³⁹H. Wilhelm, V. Zlatić, and D. Jaccard, *Physica B* **378-380**, 644 (2006).
- ⁴⁰C. H. Booth, M. Daniel, R. E. Wilson, E. D. Bauer, J. N. Mitchell, N. O. Moreno, L. A. Morales, J. L. Sarrao, and P. G. Allen, *J. Alloys Compd.* **444-445**, 119 (2007).
- ⁴¹D. Huo, J. Sakurai, T. Kuwai, Y. Isikawa, and Q. Lu, *Phys. Rev. B* **64**, 224405 (2001).
- ⁴²M. A. Continentino, S. N. de Medeiros, M. T. D. Orlando, M. B. Fontes, and E. M. Baggio-Saitovitch, *Phys. Rev. B* **64**, 012404 (2001).
- ⁴³A. P. Pikul, D. Kaczorowski, T. Plackowski, A. Czopnik, H. Michor, E. Bauer, G. Hilscher, P. Rogl, and Yu. Grin, *Phys. Rev. B* **67**, 224417 (2003).
- ⁴⁴C. D. Bredl, F. Steglich, and K. D. Schotte, *Z. Phys. B* **29**, 327 (1978).
- ⁴⁵J. A. Blanco, M. de Podesta, J. I. Espeso, J. C. Gómez Sal, C. Lester, K. A. McEwen, N. Patrikios, and J. Rodríguez Fernández, *Phys. Rev. B* **49**, 15126 (1994).
- ⁴⁶H. Yashima, H. Mori, N. Sato, and T. Satoh, *J. Magn. Magn. Mater.* **31-34**, 411 (1983).
- ⁴⁷K. A. McEwen, J.-G. Park, A. J. Gipson, and G. A. Gehring, *J. Phys.: Condens. Matter* **15**, S1923 (2003).
- ⁴⁸D. J. Newman and B. Ng, *Crystal Field Handbook* (Cambridge University Press, Cambridge, 2000).
- ⁴⁹W. T. Carnall, *J. Chem. Phys.* **96**, 8713 (1992).
- ⁵⁰D. A. Varshalovich, A. N. Moskalev, and V. K. Khersonskii,

Quantum Theory of Angular Momentum (World Scientific, Singapore, 1988).

⁵¹K. H. J. Stevens, Proc. Phys. Soc. London **65**, 209 (1952).

⁵²N. Magnani, P. Santini, G. Amoretti, and R. Caciuffo, Phys. Rev.

B **71**, 054405 (2005).

⁵³C. Rudowicz and R. Bramley, J. Chem. Phys. **83**, 5192 (1985).

⁵⁴J. D. Thompson, N. J. Curro, T. Park, E. D. Bauer, and J. L. Sarrao, J. Alloys Compd. **444**, 19 (2007).